

Two-dimensional tracking of a motile micro-organism allowing high-resolution observation with various imaging techniques

H. Oku

JST PRESTO, Kawaguchi-shi, Saitama 332-0012, Japan

N. Ogawa and M. Ishikawa

Graduate School of Information Science and Technology, University of Tokyo, Tokyo 113-8656, Japan

K. Hashimoto

Graduate School of Information Sciences, Tohoku University, Sendai-shi, Miyagi 980-8579, Japan

(Received 29 September 2004; accepted 13 December 2004; published online 2 February 2005)

In this article, a micro-organism tracking system using a high-speed vision system is reported. This system two dimensionally tracks a freely swimming micro-organism within the field of an optical microscope by moving a chamber of target micro-organisms based on high-speed visual feedback. The system we developed could track a paramecium using various imaging techniques, including bright-field illumination, dark-field illumination, and differential interference contrast, at magnifications of 5 times and 20 times. A maximum tracking duration of 300 s was demonstrated. Also, the system could track an object with a velocity of up to 35 000 $\mu\text{m/s}$ (175 diameters/s), which is significantly faster than swimming micro-organisms. © 2005 American Institute of Physics. [DOI: 10.1063/1.1857632]

I. INTRODUCTION

Continuous observation of individual motile micro-organisms is difficult, since their swimming speed is fast compared with their diameters. In fact, some bacteria can swim as fast as 50 diameters/s;¹ this corresponds to 324 km/h on the human scale for a human body 1.8 m in length. At this speed, micro-organisms can quickly go out of the range of static measurement instruments, such as the field of view of optical microscopes.

Biologists have developed various methods to solve this problem, including: (i) Securing sufficient time for observation by enlarging the field of view, and (ii) tracking a target micro-organism to keep it within the measurement range by developing special instruments.

As an example of method (i), Strickler developed an instrument having a large field of view using a Schlieren optical configuration² to observe the three-dimensional trajectory of motile micro-organisms with a fixed video camera.³ However, it was difficult to attain high optical resolution with this configuration, and, consequently, detailed observation of the target was difficult.

The alternative method (ii) is to track the target micro-organism. Berg¹ developed a tracking system of *E. coli* based on an optical microscope. This system measured the target position using a quadrant photodetector (PD) connected to the image plane of an optical microscope by optical fibers. Using this instrument, Berg *et al.*⁴ measured the three-dimensional trajectories of *E. coli*. However, this instrument was specially designed for *E. coli*, that is, the fibers were placed with a certain spacing based on the size of *E. coli* and signal processing circuits were designed for its specific visual condition, and was thus limited in terms of its observa-

tion conditions, such as illumination and magnification. Thus, this instrument lacks versatility.

In this article, we report a new micro-organism tracking system that was developed to observe “galvanotaxis” of paramecia;^{5,6} galvanotaxis is an intrinsic locomotor response toward or away from an external electrical stimulus. For our application, continuous measurement of the position and orientation of individual paramecia for a duration of at least 60 s is required. To accurately measure the orientation, high-resolution images must be acquired. Also, our system is required to work with various imaging techniques, since the most suitable imaging technique depends on the purpose of the measurement. Hence, the required specifications for our new system are (i) at least 60 s continuous observation, (ii) high-resolution images, and (iii) operation with various imaging techniques.

II. VISUAL FEEDBACK

The optical microscope is an important instrument to measure the motion of small micro-organisms, since it can measure them with adequate resolution in a noncontact manner. By using it with various imaging techniques, it has the ability to observe, for example, phase objects; micro-organisms belong to this category. However, optical microscopes cannot observe such motile targets continuously because of their limited field of view.

This problem can be solved by tracking the micro-organism within the field of view by moving the chamber of the micro-organism. In principle, this tracking can be realized by visual feedback control using a vision system mounted on the microscope. In this method, the position of the chamber is controlled based on the visual information captured by the vision system so as to keep the target within

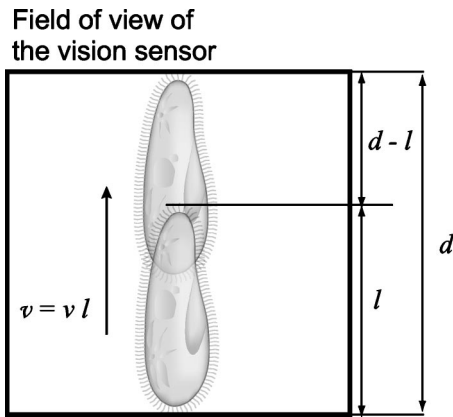


FIG. 1. Schematic diagram showing the relationship between the size of the field of view and the swimming velocity of the target micro-organism.

the field of view. This method allows continuous observation with high resolution and can be used with various imaging techniques by modifying its image-processing program.

However, conventional vision systems, such as charge coupled devices (CCDs), operate at standard video rates [30 Hz for national television standards committee (NTSC) or 24 Hz for phase alternation by line (PAL)] and are, therefore, too slow for this application. Because motile micro-organisms can swim very quickly, they can go out of the field of view of the vision system within a fraction of a second. For example, assuming that one target with a swimming speed of 50 diameters/s is magnified to fill the field of view, it will swim out in $1/50$ s, which is shorter than the frame period of such vision systems. Although such micro-organisms can be observed continuously with a large field of view using low optical magnification, in this case, detailed observation cannot be achieved. This means there is a trade-off between the size of the field of view and the resolution of the observation. This trade-off depends on the frame rate of the vision system.

Consider the observation of a micro-organism with diameter ℓ (>0) and swimming velocity v . A vision sensor coupled with an optical microscope observes this micro-organism in a field of diameter d , as shown in Fig. 1. The maximum duration t for the microorganism to pass across the field is

$$t = \frac{d - \ell}{v}. \quad (1)$$

Assuming that the vision system must acquire at least two frames to measure its dynamic motion within this period, the minimum frame rate f is

$$f = \frac{\ell/d}{1 - \ell/d} v, \quad (2)$$

where v is the relative velocity in terms of the body diameter ($v = v\ell$). The ratio ℓ/d is close to 1 when the image of the microorganism is magnified to fit the field. Thus, ℓ/d indicates the resolution of the observation. This ratio must satisfy $\ell/d \leq 1$, otherwise the magnified image will exceed the field size. The minimum frame rate f monotonically increases with ℓ/d when ℓ/d satisfies $0 < \ell/d < 1$.

To determine the frame rate, we assume a relative swimming velocity $v = 50$, and ℓ/d must satisfy $4/5 \leq \ell/d$. This condition gives $200 \leq f$. Thus, the minimum frame rate f is 200 fps. This is obviously higher than the conventional video rate. Therefore, vision systems with a high frame rate are essential for micro-organism tracking. In practice, accurate control of ℓ/d is difficult, because it depends on the target cell-size ℓ that varies between individual specimens. Considering margin of ℓ , the frame rate of 1000 fps or more is desirable.

III. HIGH-SPEED VISION SYSTEM: I-CPV

As described above, a vision system with high frame rate is essential for the tracking of micro-organisms. As our high-speed vision system, we adopted the so-called I-CPV system developed by Hamamatsu Photonics K. K.⁷ This is composed of a column parallel vision (CPV) system⁸ and an image intensifier. A block diagram of the I-CPV is shown in Fig. 2.

The CPV system captures and processes an eight-bit gray-scale image with 128×128 pixels at 1 kHz frame rate. It has a 128×128 PD array and the same number of programmable processing elements (PEs). Each PE is based on the S³PE architecture,⁹ which adopts single-instruction multiple-data stream (SIMD)-type program control. The CPV system can process image data completely in parallel. Each PE is connected with a summation circuit, so that it can extract global image features such as moments. With this structure, the CPV can execute image acquisition and various image processing operations, including feature extraction, within 1 ms.

The sensitivity of the PD array is not high because its exposure time is limited to 1 ms. However, vision systems for microscopes should have high sensitivity, since the light intensity of microscope images tends to be relatively low. To overcome this problem, the I-CPV has an image intensifier that can amplify the input image intensity several thousand

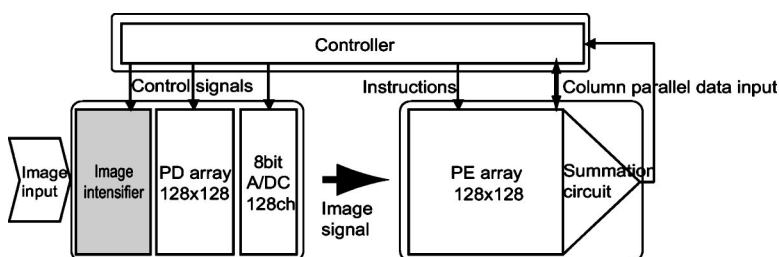


FIG. 2. Schematic diagram of I-CPV system.

TABLE I. Specifications of image intensifier in I-CPV system.

Photocathode	Multialkali (350–900 nm)
Phosphor screen	P43 (10% fall time=1 ms)
Size	18 mm square
Gate time	100 ns (min 3 ns)

times; its specifications are shown in Table I. Therefore, the I-CPV system is suitable for use as the high-speed vision system for micro-organism tracking.

IV. SPECIFICATIONS AND EXPERIMENTAL SETUP

A. Specifications

We will now discuss the specifications of a micro-organism tracking system to two dimensionally track a freely swimming target micro-organism within the field of an optical microscope by moving the micro-organism's chamber. This mechanism needs four components: (1) A high-speed vision system, (2) an XY automated stage to actuate the chamber, (3) a control processor, and (4) an optical microscope. The specifications for each component are listed below.

- (1) High-speed vision system: The high-speed vision system should be able to: (i) Acquire and process images every 1 ms, and (ii) have adequate sensitivity for microscope images with low luminance.
- (2) XY Automated stage: The XY automated stage should have: (i) High resolution, and (ii) high mobility to respond to the motion of a micro-organism.
- (3) Control processor: The control processor should have adequate processing power to conduct tracking control of the XY stage sufficiently quickly based on image features transmitted from the high-speed vision system.
- (4) Optical microscope: The microscope should (i) Have adequate resolution for measurements of microorganisms, and (ii) provide various imaging techniques, such as dark-field (DF) illumination and differential interference contrast (DIC).

TABLE II. Specifications of the XY automated stage.

Specifications	X axis	Y axis
Stroke	25 mm	25 mm
Weight of moving part	1.25 kg	0.25 kg
Maximum force per unit current	14 N/A	7.8 N/A
Resolution	1 μm	1 μm

B. System setup

Based on the specifications above, a microscope-based micro-organism tracking system has been developed. This system was designed to track *Paramecium caudatum*, a kind of protozoa. A photograph of the system and its connections are shown in Fig. 3.

The I-CPV system, which was adopted as the high-speed vision system, is mounted on a microscope. It captures and processes magnified images, and extracts image features. The control processor controls the XY stage position to track a target micro-organism within the field based on the image features.

LAL00-X70 (SMC) was adopted as the XY automated stage; its specifications are shown in Table II. Each axis has a linear coil actuator consisting of a linear core and a movable coil. The coil is combined with a moving part of the XY stage so that the part can be actuated along the core by applying current to the coil. This structure provides quick mobility. Also, this stage has an encoder with a resolution of 1 μm , almost the same as the resolution of the optical microscope.

BX50WI (OLYMPUS) was adopted as the optical microscope. This upright microscope has adequate optical magnification and provides various imaging methods, such as DF illumination and DIC. Thus, this microscope meets the required specifications. This microscope has two ports for cameras. The I-CPV system and a CCD camera were mounted on these ports so that the operator could monitor the images acquired by the high-speed vision system.

A personal computer (PC) with a Celeron 1.80-GHz pro-

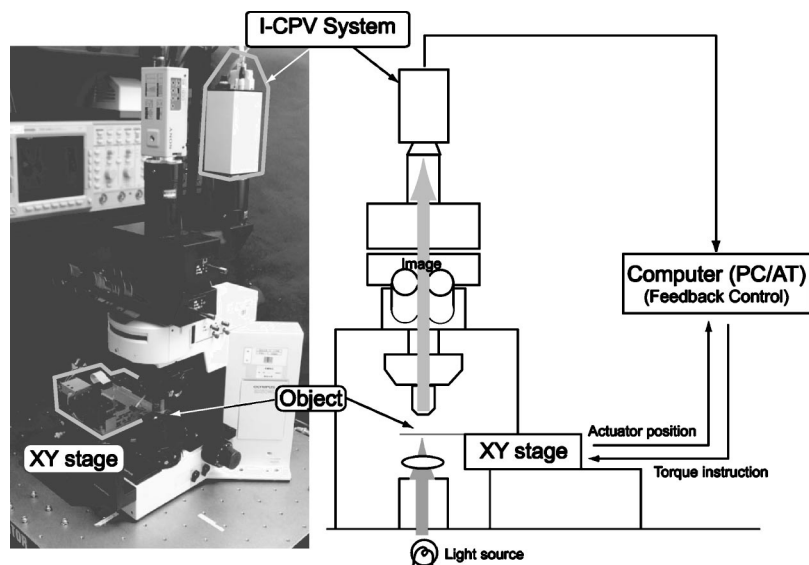


FIG. 3. Photograph and block diagram of the developed microscope-based micro-organism tracking system.

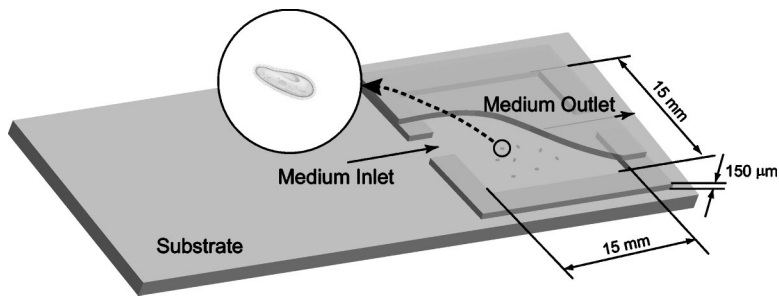


FIG. 4. Schematic figure of the chamber for the paramecia. This chamber was made of glass.

cessor and running a real-time operating system (OS) (ART-Linux, Moving Eye) was adopted as the control processor. This PC could perform the tracking control in 1 ms.

C. Chamber for micro-organisms

This system cannot track a micro-organism swimming along the optical axis of the microscope. Therefore, to prevent axial movement, a special chamber with a low depth was fabricated.

The chamber was designed for paramecia whose body length ranges from 100 to 200 μm . The chamber was a small tank with dimensions 15 mm \times 15 mm \times 150 μm . Figure 4 shows the structure of the chamber. The target paramecia were put in the chamber, together with a medium. The chamber was made of a glass slide and cut cover glasses that were bonded together using optical glue. It was fixed on the XY stage so that its horizontal position could be controlled in two dimensions by the control PC.

D. Image processing

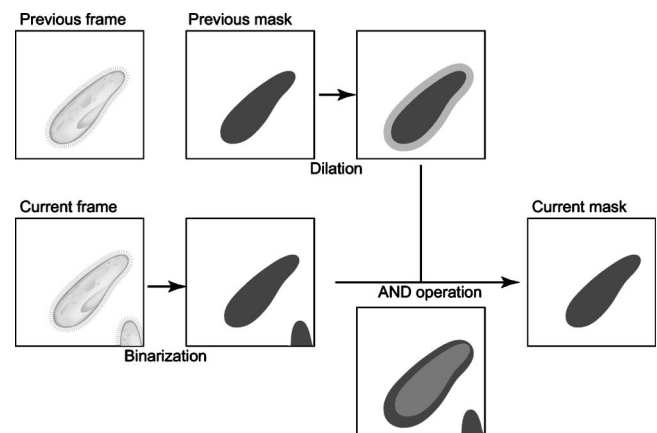
For every image, the I-CPV system extracted: (a) The area of objects, (b) the target micro-organism among the objects, and (c) the position and the tilt angle of the target in this order. Procedure (b) is required when several micro-organisms are in the field of the I-CPV system. In this case, the I-CPV system needs to extract one tracking target from two or more objects.

(a) The method used to extract the area of objects differed depending on the imaging mode. In this article, three kinds of imaging methods, bright-field (BF) illumination, DF illumination, and DIC, were considered. Methods to extract the area of objects for these illuminations are described below.

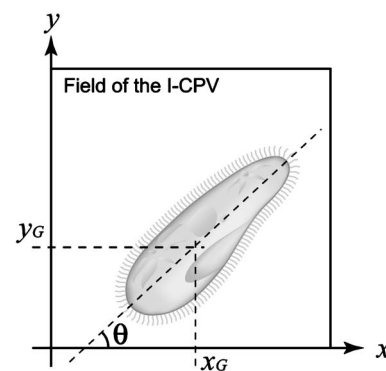
- (1) In the case of BF illumination, objects are shown in black on a white background. Thus, black areas were extracted as objects using a given threshold.
- (2) In the case of DF illumination, objects are shown in white on a black background. Thus, white areas were extracted as objects using a given threshold.
- (3) In the case of DIC, the background is gray. Areas where the object's spatial phase distribution is not constant become white or black. Therefore, areas whose light intensity is different from the background by more than a given threshold were extracted as objects. Even if the object has areas in which the phase distribution is constant, these areas do not cover its whole body. However, micro-organisms rarely have such a distribution. Moreover, the purpose of this image processing is to extract

overall features, such as position and orientation, which are not sensitive to detailed partial information.

(b) The self-windowing algorithm proposed by Ishii *et al.*¹⁰ was adopted to extract an individual target from the objects. This algorithm uses a one-bit mask that covers the target. Figure 5(a) shows how this algorithm updates its mask. When a new image is acquired, a new mask is calculated by performing an AND operation between a dilated version of the previous mask and a binarized version of the new image. Thus, the mask tracks the nearest object from the previous target. This process works well since the target moves very little between two consecutive frames at high frame rate. An initial mask is generated when only one target exists within the field.



(a)



(b)

FIG. 5. (a) The self-windowing algorithm. This algorithm updates its mask based on the previous mask and the binarized current image. (b) Image features extracted by the I-CPV.

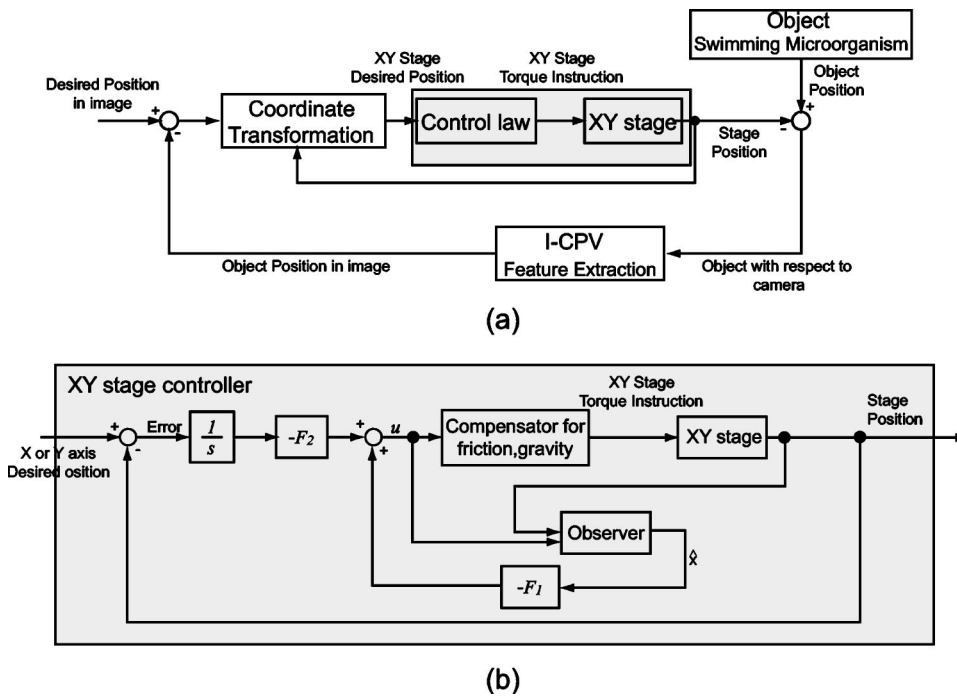


FIG. 6. Block diagram of the tracking controller, showing (a) the entire visual servocontroller and (b) the position controller of the XY stage, which is included in the gray box in (a).

When a target and another object collide and then divide again, the I-CPV system should determine which object was the previously tracked target. Although this algorithm includes methods to detect collision and division, identification of objects is beyond the scope of the algorithm. In this article, we neglected this case.

(c) Figure 5(b) shows image features extracted by the I-CPV system. The target position (x_G, y_G) and the tilt angle θ were calculated using the zeroth, first, and second moments of the mask described above. Moments of image M are defined as

$$M_{m,n} = \sum_x \sum_y x^m y^n I(x,y), \quad (3)$$

where x and y are coordinates in the image and $I(x,y)$ is the intensity at pixel (x,y) .

The centroid of the mask (x_G, y_G) was adopted as the position of the target. The centroid position $(x_G, y_G) = (M_{1,0}/M_{0,0}, M_{0,1}/M_{0,0})$. The tilt angle of the target relative to the x axis in the image is calculated using the following relation:

$$\tan 2\theta = \frac{2\left(M_{1,1} - \frac{M_{1,0}M_{0,1}}{M_{0,0}}\right)}{\left(M_{2,0} - \frac{M_{1,0}^2}{M_{0,0}}\right) - \left(M_{0,2} - \frac{M_{0,1}^2}{M_{0,0}}\right)}. \quad (4)$$

This tilt angle was not used for the tracking control.

E. Tracking controller

Image-based visual servoing¹¹ was adopted for tracking control, as shown in Fig. 6(a). The desired position in the image was set to be the center of the field so that the target would be tracked within the field of view.

This image-based visual servoing needs a position controller for the XY stage. The design of the controller was based on a Smith–Davison servo,¹² which is based on a

mathematical model of the control target. According to the structure of the XY stage, we assumed that axes of the stage were physically independent of each other, and each axis was modeled as the following mass and damper model:

$$m \frac{d^2}{dt^2} x + \gamma \frac{d}{dt} x = u, \quad (5)$$

where m is the mass of the axis, x is the position, γ is the coefficient of dynamic friction, and u is the external force generated by the electrical current of the coil. These parameters were estimated by the stage's frequency response, measured in advance.

Figure 6(b) shows a block diagram of the position controller. The observer shown in the diagram estimates the velocity of the stage using a Kalman filter. $1/s$ is the integration operator. F_1 and F_2 are constant vectors that determine the characteristics of the controller. As a benchmark of this controller, its step response is shown in Fig. 7.

V. RESULTS

Tracking experiments were conducted with three kinds of imaging techniques, BF illumination, DF illumination, and DIC, and two magnification levels, 5 times and 20 times. Wild-type *Paramecium caudatum* cells were adopted as specimens, which were cultured at 25 °C in a soy flour solution. Cells were collected together with the solution, filtered through a nylon mesh to remove debris, washed with mineral water without gas, and infused into the chamber.

Figures 8–10 show continuous images captured by the monitoring CCD camera and trajectories of the target when the magnification was 20 times. Two-dimensional trajectories of targets were calculated from both the position of the XY stage and the object's position in the image captured by the I-CPV. (See EPAPS material for the movie of these results.)¹³

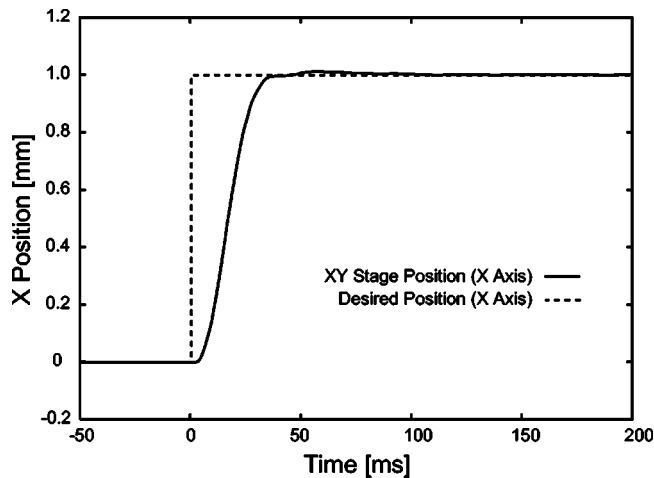


FIG. 7. Step response trajectory of the XY stage. This plot shows the response of the X axis.

As described above, the I-CPV can calculate the tilt angle. Figure 11 shows the tilt angle sequence of the paramecium with DIC and $20\times$ magnification.

Since this system moves the chamber for tracking, the force of acceleration acts on the specimens. According to the result with differential interference contrast and 20 times magnification, the standard deviation of acceleration was about 0.2 m/s^2 , and the maximum acceleration was about 1.5 m/s^2 . In our experiments, the behavior of the paramecium seemed not differ from that in the static environment without tracking.

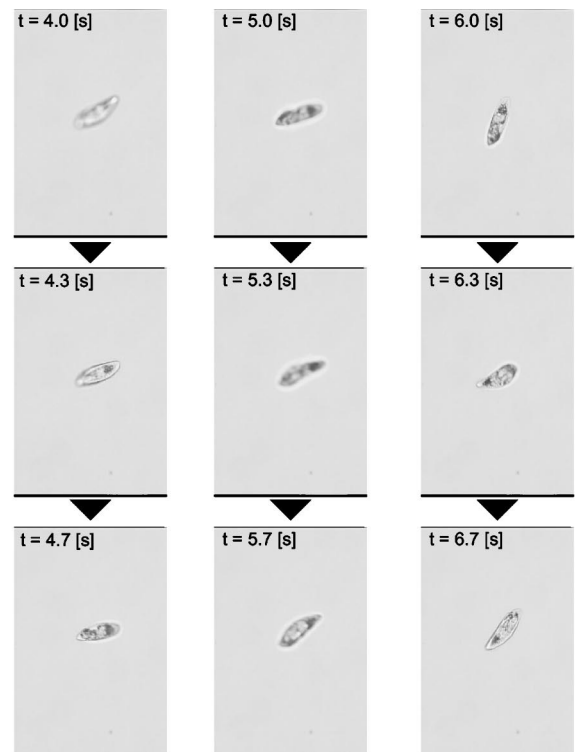
According to these results, the system we developed could track a swimming paramecium in the center of the field for more than 60 s with adequate resolution to calculate its orientation. Also, the system could work under three kinds of observation conditions. Therefore, the system satisfied the requirements discussed in the Introduction.

VI. DISCUSSION

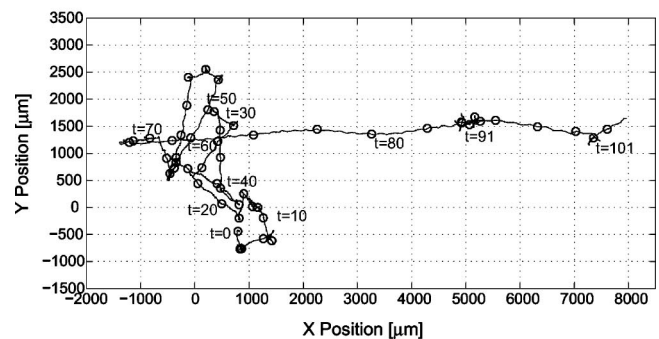
A. Target velocity limitation

As discussed above, the limitations of our system are related to the swimming velocity of the target. To estimate the limitations of our system, the maximum trackable velocity was measured. However, it is impossible to control the swimming velocity of micro-organisms. To overcome this, we approximately evaluated the velocity limitation by performing a *find and track* experiment. In this experiment, a static target was fixed on the XY stage. The XY stage was controlled to slide the target into the field of the I-CPV with a certain velocity from outside the field, as shown in Fig. 12. As soon as the I-CPV recognized the object sliding into the field, the control method was changed from sliding control to tracking control. Successful tracking suggests that the system could handle the velocity. By varying the sliding velocity, the target velocity limitation could be roughly estimated.

A transparent plastic sheet on which an ellipse was printed in black was fixed on the XY stage. The ellipse had a major axis diameter of $200 \mu\text{m}$ and a minor axis diameter of $100 \mu\text{m}$, that is, almost the same dimensions as an average paramecium. Its major axis was parallel to the sliding direc-



(a)

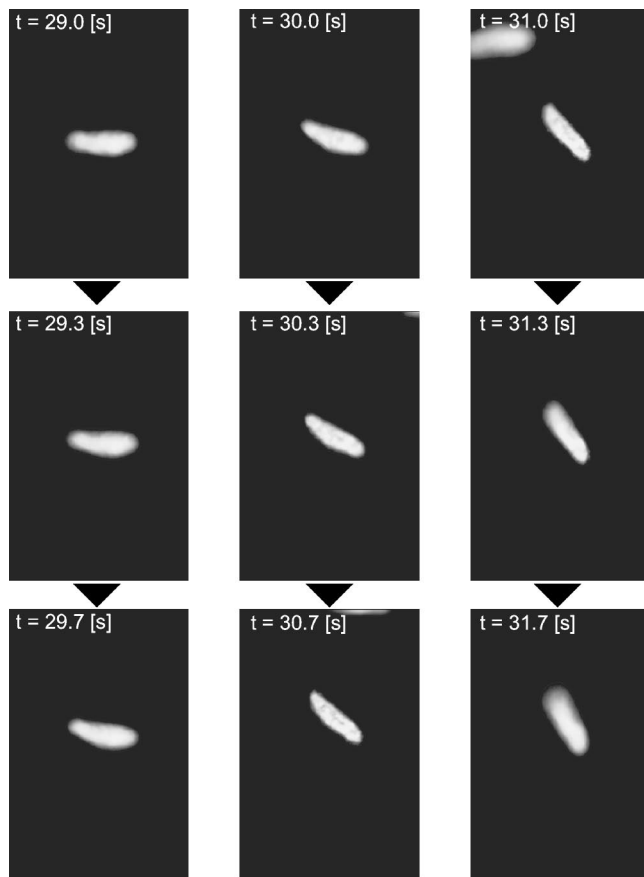


(b)

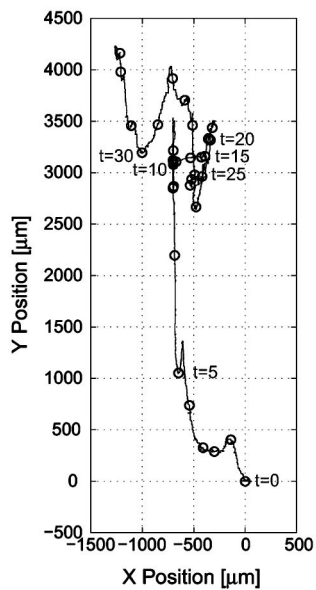
FIG. 8. Tracking experiment results with bright field illumination, $20\times$ magnification. (a) Continuous images of the target paramecium captured by the CCD camera for monitoring. (b) Trajectory of the tracked paramecium; circles are plotted at the paramecium position every 2 s.

tion. BF illumination and $20\times$ magnification were adopted. The width of the field of the I-CPV system was $256 \mu\text{m}$ in this case. In terms of the notation introduced in Sec. II, these conditions can be written as $\ell=200 \mu\text{m}$, $d=256 \mu\text{m}$, and $\ell/d \approx 4/5$.

Figure 13 shows stage trajectories at various sliding velocities. When the sliding velocity was less than or equal to $10\,000 \mu\text{m/s}$, the system could find the target and track it adequately. The sliding velocity of $10\,000 \mu\text{m/s}$ equals the velocity of 50 diameters/s that corresponds to the swimming velocity of a bacterium. At a sliding velocity of $25\,000 \mu\text{m/s}$ (corresponding to 125 diameters/s), the center of the ellipse came close to the boundary of the field, but the tracking was successful. At a sliding velocity of $40\,000 \mu\text{m/s}$ (corresponding to 200 diameters/s), the tracking was unstable. At faster sliding velocities, the tracking failed. However, the



(a)

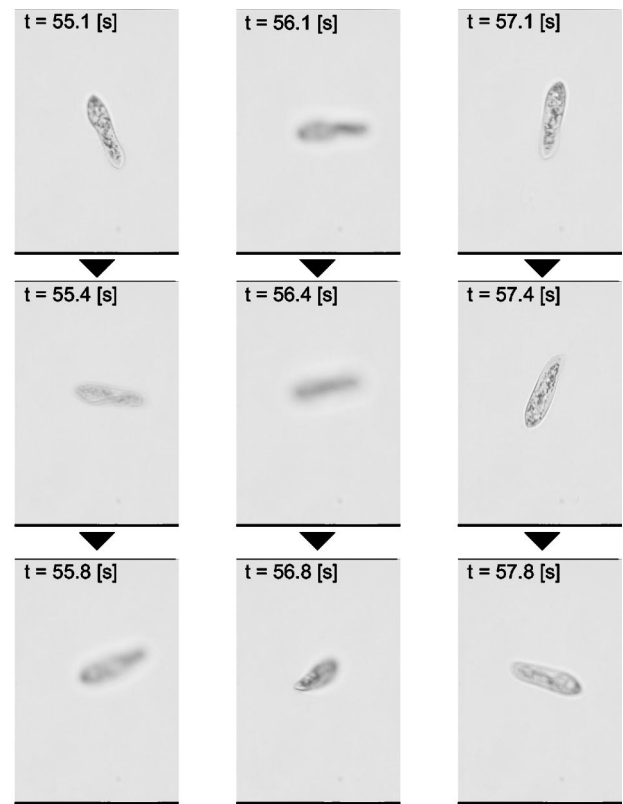


(b)

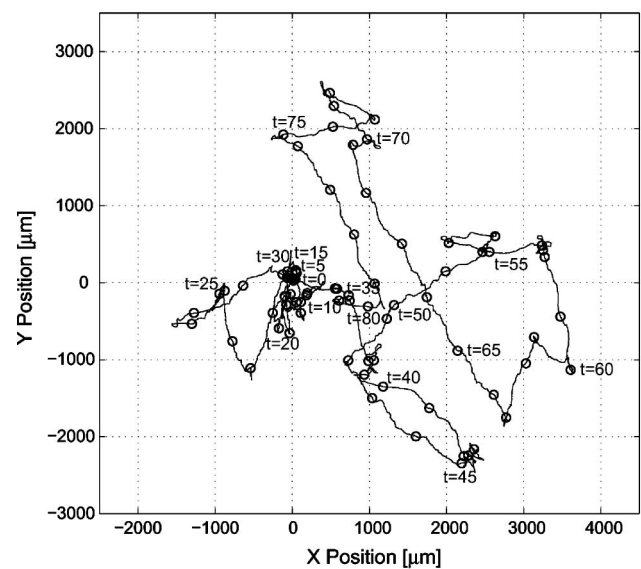
FIG. 9. Tracking experiment results with DF illumination, 20 \times magnification. (a) Continuous images of the target paramecium captured by the CCD camera for monitoring. (b) Trajectory of the tracked paramecium; circles are plotted at the paramecium position every second.

I-CPV system could still detect the object entering its field of view at these velocities.

These results suggest that the system we developed has



(a)



(b)

FIG. 10. Tracking experiment results with DIC, 20 \times magnification. (a) Continuous images of the target paramecium captured by the CCD camera for monitoring. (b) Trajectory of the tracked paramecium; circles are plotted at the paramecium position every second.

sufficient performance to track and observe micro-organisms.

B. Reason for tracking failure

Here, the reason for tracking failure will be discussed. First, the term *tracking trial* will be defined. In this article, one *tracking trial* is defined as one temporally continuous

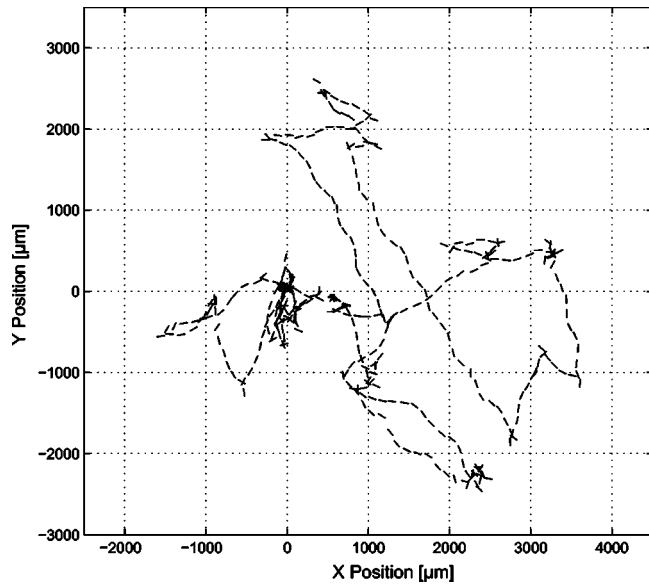


FIG. 11. Sequence of orientations of paramecium with DIC and 20× magnification. Each line shows the long axis of the paramecium. These lines are plotted at the position of the target every 0.2 s.

tracking state of one target. If the I-CPV system fails to recognize the target, the previous *tracking trial* is finished at that point. Another *tracking trial* starts when the system recovers tracking control, even if the new target is the same object as the previous target.

Table III shows the reasons for tracking failure and the number of *tracking trial* stopped by these failures. The reasons were categorized into: (1) *Recognized a number of objects*, (2) *recognized objects wrongly*, (3) *system failure*, (4) *stopped by operator*, and (5) *unknown reasons*. (1) *Recognized a number of objects* indicates that the I-CPV recognized two or more objects as one object. (2) *Recognized objects wrongly* indicates that the I-CPV erroneously observed debris or a bubble in the chamber. (3) *System failure* indicates that the target swam out of the range of the XY stage, or that tracking control became unstable because of a modeling error of the stage.

According to Table III, most failures were due to; (1) *Recognized a number of objects* (more than 80% of the time). This is because the self-windowing algorithm itself could not handle collision and division of objects, as described in Sec. IV D. Hence, the system could not handle collision adequately. We are studying a new algorithm to solve this problem now. Because of this problem, the achievable durations of *tracking trials* depended on the density of

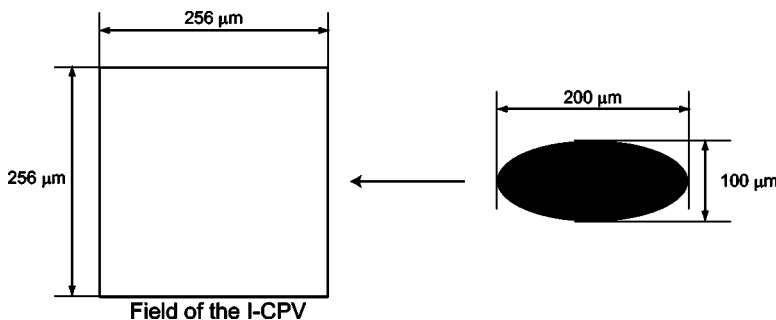


FIG. 12. Schematic figure of the configuration for measuring the limitations of the system. A target, an ellipse printed on a transparent sheet, slides into the field of the I-CPV at a certain velocity. The sheet was fixed on the XY stage so that its position could be controlled.

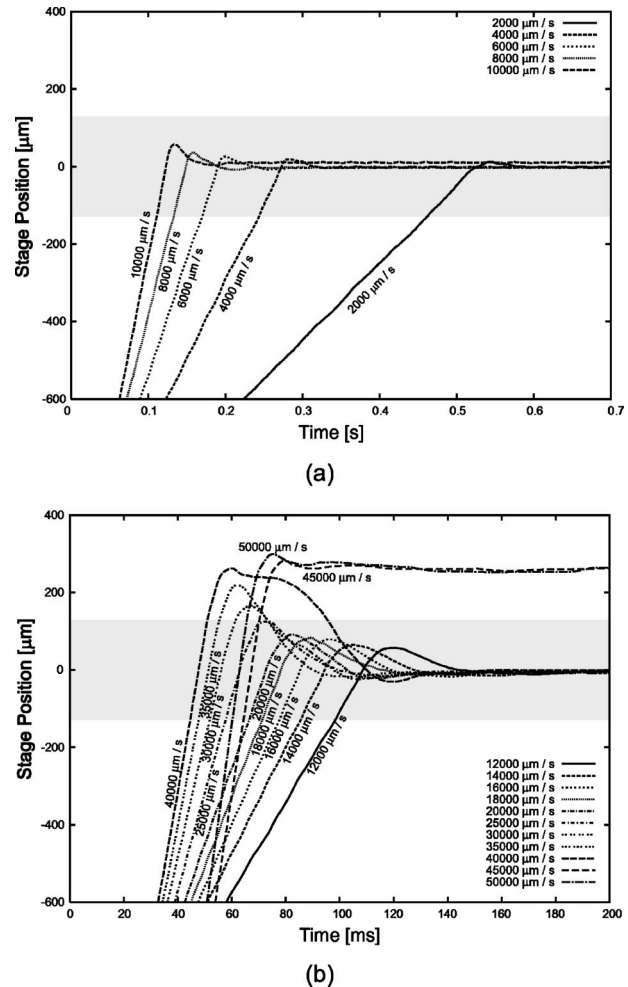


FIG. 13. Stage trajectories at various sliding velocities plotted against time. (a) Trajectories when the incoming velocity was less than or equal to 10000 $\mu\text{m/s}$, and (b) Trajectories when the velocity was faster than 10000 $\mu\text{m/s}$. When the stage position was in the shaded region, the center of the ellipse was in the field of the I-CPV.

the paramecia. The possibility of collision was high when the density was high.

In contrast, the frequencies of (3) *System failure* and (5) *Unknown reasons* were low. Therefore, the developed system worked well except for the image processing.

Maximum, minimum, and average durations of *tracking trials* are shown in Table IV. According to these results, a maximum duration of 300 s was achieved, which is sufficient to observe taxis of motile micro-organisms. The maximum duration was obtained in the case of BF illumination. However, this does not indicate the relative merits of the

TABLE III. Reasons for tracking failure and their frequency. Labels such as BF5 indicate the system configuration. BF is bright field illumination. DF is dark field illumination. DIC is differential interference contrast. The number following indicates the magnification. Numbers in parentheses show the proportion as a percentage of *tracking trials* compared with the total number of trials of the same configuration.

Reason	BF5	BF20	DF5	DF20	DIC5	DIC20	Subtotal
(1) Recognized a number of objects	13 (86%)	48 (92%)	17 (68%)	19 (82%)	15 (75%)	38 (86%)	150 (83%)
(2) Recognized objects wrongly	2 (13%)	3 (5%)	4 (16%)	1 (4%)	4 (20%)	3 (6%)	17 (9%)
(3) System failure	0	1 (1%)	2 (8%)	0	0	1 (2%)	4 (2%)
(4) Stopped by operator	0	0	0	0	0	2 (4%)	2 (1%)
(5) Unknown	0	0	2 (8%)	3 (13%)	1 (5%)	0	6 (3%)
Total	15	52	25	23	20	44	179

imaging technique, because the durations strongly depend on the density of the paramecia.

In this article, we reported on a micro-organism tracking system using a high-speed vision system. A maximum tracking duration of 300 s and measurement of the position and orientation of the specimen were achieved. Also, the system we developed demonstrated its versatility by tracking a paramecium with various imaging techniques, such as BF illumination, DF illumination, and DIC, at magnifications of 5 times and 20 times. Therefore, the system achieved the required specifications, and thus had sufficient performance to observe dynamic behavior of motile micro-organisms.

¹H. C. Berg, Rev. Sci. Instrum. **42**, 868 (1971).

TABLE IV. Maximum, minimum, and average duration of *tracking trials*. Labels BF5, etc., indicate system configuration, which are explained in the caption of Table III.

Duration	BF5	BF20	DF5	DF20	DIC5	DIC20	Total
Maximum [s]	300	229	125	84	62	184	300
Minimum [s]	1	1	3	1	2	1	1
Average [s]	48	45	32	13	13	33	31

²W. J. Smith, *Modern Optical Engineering*, 3rd ed. (McGraw-Hill, New York, 2000), p. 592.

³J. R. Strickler, Philos. Trans. R. Soc. London, Ser. B **353**, 671 (1998).

⁴H. C. Berg and D. A. Brown, Nature (London) **239**, 500 (1972).

⁵N. Ogawa, H. Oku, K. Hashimoto, and M. Ishikawa, *Proceedings of the 2004 IEEE International Symposium on Biomedical Imaging* (IEEE, New York, 2004), pp. 1331–1334.

⁶N. Ogawa, H. Oku, K. Hashimoto, and M. Ishikawa, *Proceedings of the 2004 IEEE International Conference on Robotics and Automation* (IEEE, New York, 2004), pp. 1646–1651.

⁷H. Toyoda, N. Mukohzaka, K. Nakamura, M. Takumi, S. Mizuno, and M. Ishikawa, *Proceedings of the Symposium on High-Speed Photography and Photonics 2001* (2001), Vol. 5-1, pp. 89–92 (in Japanese).

⁸Y. Nakabo, M. Ishikawa, H. Toyoda, and S. Mizuno, *Proceedings of the 2000 IEEE International Conference on Robotics and Automation* (IEEE, New York, 2000), pp. 650–655.

⁹M. Ishikawa, K. Ogawa, T. Komuro, and I. Ishii, *Digest of Technical Papers of the 1999 IEEE International Solid-State Circuits Conference (ISSCC)* (IEEE, New York, 1999), pp. 206–207.

¹⁰I. Ishii and M. Ishikawa, Syst. Comput. Japan **32**, 51 (2001).

¹¹*Visual Servoing*, edited by K. Hashimoto (World Scientific, Singapore, 1993).

¹²H. W. Smith and E. J. Davison, Proc. Inst. Electr. Eng. **119**, 1210 (1972).

¹³See EPAPS Document No. E-RSINAK-76-208503 for the movie file of the tracking experiments. A direct link to this document may be found in the online article's HTML reference section. The document may also be reached via the EPAPS homepage (<http://www.aip.org/pubservs/epaps.html>) or from <ftp.aip.org> in the directory /epaps. See the EPAPS homepage for more information.